

Evaporative cooling of metastable helium in the multi-partial-wave regime

Scott V. Nguyen,^{1,2} S. Charles Doret,^{1,2} Colin B. Connolly,^{1,2} Robert A. Michniak,^{1,2} Wolfgang Ketterle,^{2,3} and John M. Doyle^{1,2}

¹Harvard-MIT Center for Ultracold Atoms, Cambridge, Massachusetts 02138, USA

²Department of Physics, Harvard University, Cambridge, Massachusetts 02138, USA

³Department of Physics, MIT, Cambridge, Massachusetts 02139, USA

(Received 3 October 2005; published 29 December 2005)

Metastable helium is buffer gas cooled, magnetically trapped, and evaporatively cooled in large numbers. 10^{11} $^4\text{He}^*$ atoms are trapped at an initial temperature of 400 mK and evaporatively cooled into the ultracold regime, resulting in a cloud of $2 \pm 0.5 \times 10^9$ atoms at 1.4 ± 0.2 mK. Efficient evaporation indicates low collisional loss for $^4\text{He}^*$ in both the ultracold and multi-partial-wave regime, in agreement with theory.

DOI: [10.1103/PhysRevA.72.060703](https://doi.org/10.1103/PhysRevA.72.060703)

PACS number(s): 34.50.-s, 03.75.-b, 39.10.+j

The achievement of quantum degeneracy in dilute atomic gases has revolutionized the field of atomic physics. It has enabled a host of scientific explorations [1] including coherent atom and molecular optics [2,3], nonlinear atom optics [4,5], the observation of superfluidity in atomic gases [6,7], and the study of novel quantum systems [8,9]. Almost all of these studies used alkali-metal atoms. However, metastable helium $^4\text{He}^*$, first Bose-condensed in 2001 [10,11], has the unique property that single-atom detection can be performed with high temporal and spatial resolution using multichannel plates. By comparison, single-atom detection of alkali-metal atoms using multiple-photon scattering in a magneto-optical trap [12] or in high-finesse optical cavities offers only limited spatial resolution [13] and single-channel detection. Therefore, $^4\text{He}^*$ may become the work horse for quantum atom optics, where in analogy with quantum optics [14], the statistics and correlations of single particles are studied. For example, recently $^4\text{He}^*$ was used for three-dimensional correlation measurements in both thermal clouds and Bose-Einstein condensates, the atomic analog to the Hanbury-Brown Twiss experiment [15].

Experiments to produce Bose-Einstein condensates of $^4\text{He}^*$ have thus far used laser cooling as the initial loading stage. However, the number of $^4\text{He}^*$ atoms capable of being loaded into a magnetic trap is limited by both the low efficiency for exciting helium to the metastable state and the lower scattering rate of the 1083 nm cooling transition as compared to the transitions used in cooling the alkali-metals. The experiments reported in Refs. [10,11] started with 10^8 laser cooled atoms, and after evaporation achieved Bose-Einstein condensates with 10^5 atoms, much smaller than typical numbers achieved with alkali-metal atoms. More recently, an optimized laser cooling scheme including collimation, deflection, slowing, and trapping stages improved the number of atoms loaded into the magnetic trap tenfold [16]. Further increasing the number of atoms initially trapped would lead to larger condensates and facilitate new experiments in quantum atom optics.

Here we present a radically different approach to obtaining ultracold $^4\text{He}^*$ atoms based on cryogenic buffer gas loading, a method shown to be capable of cooling and magnetically trapping a variety of atoms and molecules in large

numbers (for example, Cr [17], Dy, Ho [18], CaH [19], and NH [20]). In the case of Cr, more than 10^{12} atoms were magnetically trapped, a number limited solely by the production efficiency. Because it operates at ~ 0.5 K, buffer gas loading is sensitive to collisional physics in the multi-partial-wave regime. This is in contrast to laser cooling where collisions occur only after the atoms have reached the ultracold regime. In the case of $^4\text{He}^*$ at 0.5 K, collisional dynamics depend on the lowest seven partial waves. Additionally, $^4\text{He}^*$ is susceptible to Penning ionization; although the theory of $^4\text{He}^*$ collisions has been verified in the ultracold regime, it was an open question as to whether Penning ionization would be similarly suppressed at higher temperatures and magnetic fields as it was at low temperatures and fields.

In this extension of buffer gas loading to a metastable species, 10^{11} $^4\text{He}^*$ atoms were loaded directly from a dilute He vapor within the trapping region and evaporatively cooled from the initial loading temperature of 400 mK to 1.4 ± 0.2 mK with $2 \pm 0.5 \times 10^9$ $^4\text{He}^*$ atoms remaining. This approach could easily be extended to $^3\text{He}^*$ - $^4\text{He}^*$ mixtures. This work represents a major advance in buffer gas loading, overcoming previous technical and collisional problems, cooling the atoms through the multi-partial-wave regime into the ultracold regime with an increase in phase space density of five orders of magnitude from the initial loading conditions.

The apparatus, shown in Fig. 1, is similar to that described in Ref. [21]. A double-walled plastic cell, maintained at 0.4 K by a ^3He refrigerator via a superfluid liquid helium thermal link, sits coaxially inside the bore of a superconducting anti-Helmholtz magnet, creating a spherical quadrupole trap with depths up to 3.67 T. This electrically insulating cell allows the magnetic trapping fields to be changed rapidly without inducing undesirable eddy currents. A valve separates the trapping region from a pumping region filled with 30 g of activated charcoal maintained at a temperature of 1.5 K. This charcoal has a very high pumping speed of 100 l/s.

In previous implementations of buffer gas loading, the trapping region was filled through a thin fill line with helium buffer gas to a density of $\sim 10^{16}$ cm^{-3} . Atoms produced via laser ablation thermalized with the cold buffer gas and were

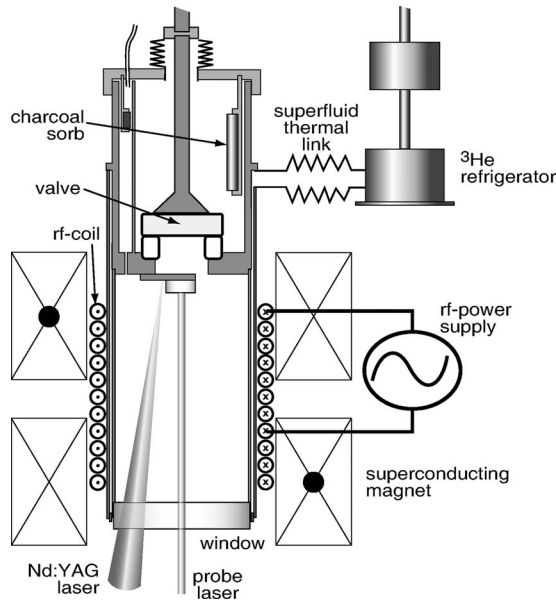


FIG. 1. Cross-sectional schematic of the experimental apparatus. $^4\text{He}^*$ is generated from a helium film by an rf-discharge and a Nd:YAG laser pulse and loaded into the superconducting magnetic trap.

subsequently trapped. The valve was then opened, and the buffer gas was pumped onto the charcoal sorb, leaving behind a thermally isolated trapped sample. Although this removed the bulk of the buffer gas from the trapping chamber, the desorption of ^4He atoms from a film that coats the cell walls provided an influx 10^{12} ^4He atom/s into the cell volume, resulting in a roughly constant background gas density of $\sim 10^{10}$ cm^{-3} . At this density, the loss rate from collisions with background ^4He gas was too high for efficient evaporation. This film could be thinned by “baking out” the cell, i.e. by bringing the temperature of the cell up to 650 mK while the atoms remained trapped. Although this lowered the background gas levels, it worked only for species with large magnetic moments such as chromium ($6\mu_B$) [21]. A $2\mu_B$ species, like $^4\text{He}^*$, is blown out of the trap by the hot helium during such a bake out procedure.

In this experiment with $^4\text{He}^*$, the problems associated with the desorbing helium film are greatly mitigated by a different scheme to produce and load $^4\text{He}^*$ into the magnetic trap. The experiment begins by filling the cell to a density of $\sim 10^{15}$ cm^{-3} with the valve initially closed. After a short wait while the ^4He gas comes into equilibrium with the cell, the valve is opened. The ^4He gas is pumped away, leaving behind a ^4He film that coats the cell walls and is the source of unwanted background gas. The cell is then heated to 700 mK for 30 s, driving weakly bound monolayers off the film. The remaining few monolayers are more tightly bound to the surface, lowering the effective vapor pressure and reducing the background density to $< 10^6$ cm^{-3} . At this density, the loss rate from collisions with background ^4He gas is negligible. With the “prepared” cell, $^4\text{He}^*$ is produced in a glow discharge in the trapping region. The discharge is initiated by sending a 100 μs 10 W rf pulse at 118 MHz through a helical coil surrounding the cell. A 1 mJ laser pulse from a

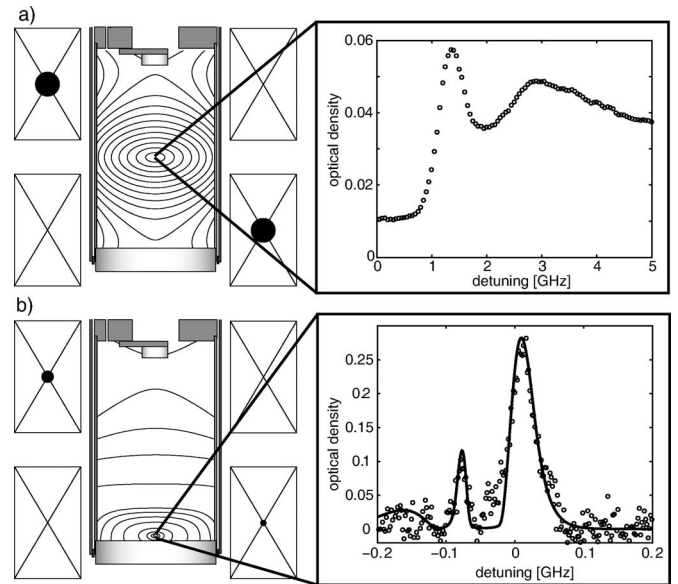


FIG. 2. Trapping and evaporative cooling of $^4\text{He}^*$. (a) The magnetic field contour lines at the initial trap depth $U_{\text{trap}} = 4.9$ K. Inset: spectrum of trapped $^4\text{He}^*$ initially loaded at 0.4 K. (b) The contour lines at the end of the evaporation, $U_{\text{trap}} = 2.7$ mK. Inset: spectrum of trapped $^4\text{He}^*$ after evaporation. The fit (solid line) gives $T = 1.4 \pm 0.2$ mK, $n_0 = 2.3 \pm 0.2 \times 10^{12}$ cm^{-3} , and $N = 2 \pm 0.5 \times 10^9$.

frequency-doubled Nd:YAG laser coincident with the rf pulse helps reliably ignite the discharge. The $^4\text{He}^*$ atoms are detected via laser absorption spectroscopy on the $^3S_1 \rightarrow ^3P_2$ transition at 1083 nm.

At a trap depth of 3.67 T ($U_{\text{trap}} = 4.9$ K), roughly 10^{11} $^4\text{He}^*$ atoms in the fully stretched state $|S=1, m_S=+1\rangle$ are trapped at peak densities of 10^{11} cm^{-3} [Fig. 2(a)]. While other m_S states are also likely to be produced in the discharge, they would be lost to diffusion and Penning ionization too rapidly to be detected by our scheme. Given typical rf discharge efficiencies of 10^{-5} [22], the number of $^4\text{He}^*$ observed in the trap implies an initial ^4He density in the cell of $> 10^{14}$ cm^{-3} , a number far too large to be accounted for by the equilibrium background ^4He density in the cell. We believe the source of this large density is rapid desorption of ^4He atoms from the cell walls due to local heating of the cell by the rf pulse; after this initial large influx of the atoms, those atoms not converted into $^4\text{He}^*$ and trapped are cryopumped back to the cell walls with a time constant of ~ 1 ms. Although this method of producing $^4\text{He}^*$ reduces the number of atoms initially produced by roughly an order of magnitude compared to using a buffer gas filled cell, it reduces the background gas density sufficiently to enable efficient evaporative cooling.

When the $^4\text{He}^*$ are initially loaded, the trap depth U_{trap} is set by the cell walls. Utilizing independent control of the currents in the two coils, $^4\text{He}^*$ is evaporated by lowering the trap sample towards the surface of the cell window [Fig. 2(b)]. Atoms that hit the window are lost through adsorption. As the atoms at the edge of the cloud have higher energy than the average energy of an atom in the cloud, evaporative cooling occurs. This adsorption method has been previously demonstrated with both H and Rb [23,24]. In this method,

the trap depth is decoupled from the confinement, an advantage over simply lowering the depth of the trap uniformly. Here the trap depth is determined by the distance between the trapped sample and the cell window, set by the ratio of the two coil currents, whereas the confinement is set by the magnitude of the bottom coil current. This allows for tight confinement and, therefore, higher $^4\text{He}^* - ^4\text{He}^*$ collision rates. The trap shape is only minimally affected during this evaporation procedure.

The evaporation trajectory starts with the trapped sample 5 cm ($U_{\text{trap}} = 4.9$ K) from the cell window. The radial (axial) gradient is 1.15 (2.3) T/cm. Over 180 s, the trap center is gradually ramped towards the window to a final separation of $580\text{ }\mu\text{m}$ (2.7 mK) and radial (axial) gradient of 200 (400) Ga/cm, resulting in a trapped sample of $N = 2 \pm 0.5 \times 10^9$ $^4\text{He}^*$ atoms with a peak density of $n_o = 2.3 \pm 0.2 \times 10^{12}\text{ cm}^{-3}$ and temperature of $T = 1.4 \pm 0.2$ mK [Fig. 2(b)]. N , n_o , and T are determined by fitting the trapped atoms' Zeeman-broadened absorption spectrum to that of a spatial Boltzmann distribution of atoms in our magnetic trap, as described in Refs. [25,26]. The evaporation trajectory was empirically optimized, and we observed that during most of the evaporation, the ratio of the trap depth to the temperature defined as $\eta \equiv \mu_B B / k_B T$ was ~ 5 . Only during the final stages of evaporation down to ~ 1 mK was this ratio observed to be reduced to 2. At the coldest temperature of 1.4 mK, the corresponding phase space density is 3×10^{-5} , an increase of 5 orders of magnitude over the initial loading conditions. The efficiency of the evaporation implies a favorable ratio of elastic to inelastic cross sections in the multi-partial-wave regime, confirming the calculation of Shlyapnikov and co-workers [27,28].

As expected in a quadrupole trap, further evaporation is ultimately limited by Majorana flops (nonadiabatic spin flips to untrapped states) from the magnetic field zero at the center of our quadrupole trap. At the coldest temperatures, the trap lifetime decreases from hundreds of seconds to just a few seconds. Previous studies showed that the loss rate due to Majorana flops is set by the ratio of the surface area of the nonadiabatic region to surface area of the atomic cloud [29,30]. By varying the evaporation trajectory we measure the trap lifetime at different temperatures and confinements (Fig. 3). For a cloud size with a spatial extent of $d \equiv 2k_B T / \mu_B B'$, where B' is the average gradient of the quadrupole trap, we estimate a lifetime of $\tau = 12.4 d^2\text{ s/mm}^2$, agreeing well with the measured values.

The number of atoms obtained here at 1 mK using buffer gas loading is already comparable to or better than the best efforts obtained using laser cooling, implying that further evaporation towards quantum degeneracy should be very efficient. However, this will require the atoms be transferred into an Ioffe trap to avoid Majorana flops. This can be achieved by adding a third coil at the cell window oriented perpendicular to the cell axis (QUIC trap [31]). The final stage of evaporation towards quantum degeneracy can be further enhanced by using the standard method of rf evapo-

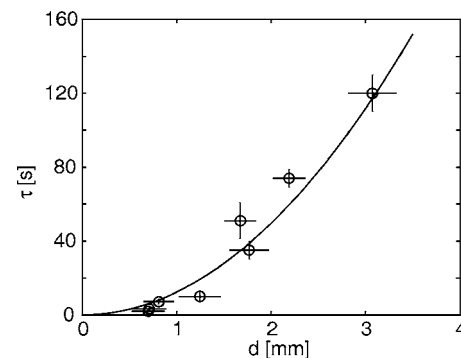


FIG. 3. Trap loss due to Majorana flops. The open circles are measured trap lifetimes at various temperatures and trap confinements. The solid line is an estimation of the trap lifetime due to Majorana flops for a cloud of size d .

ration. An evaporation model indicates that for our initial number and density, a Bose-Einstein condensate of $>10^7$ $^4\text{He}^*$ should be achievable, two orders of magnitude larger than previously reported [10,11,32] and comparable to the number of condensate atoms achieved with alkali-metal species. Furthermore, the numbers achieved in our first demonstration of buffer gas loading of $^4\text{He}^*$ were not optimized. For example, in an improved cryostat that is able to attain lower cell temperatures, it should be possible to load the trap at 400 mK with 100 times more helium atoms and then control the desorption of atoms from the helium film by lowering the cell temperature, resulting in at least a tenfold increase in the number of trapped $^4\text{He}^*$. Our present results indicate that the same improved cryostat should also lead to major improvements in the number trapped and evaporatively cooled for other atomic species with magnetic moments of $\geq 2\mu_B$ (and perhaps as low as $1\mu_B$).

A major advantage of buffer gas loading over laser cooling is that multiple species can be trapped without an increase in experimental complexity [33]. The extension of our method to $^3\text{He}^*$ and $^3\text{He}^* - ^4\text{He}^*$ mixtures should be straightforward. However, in contrast to $^4\text{He}^*$, there exists no calculations of inelastic cross sections for $^3\text{He}^* - ^3\text{He}^*$ collisions. It is an open question whether the hyperfine structure of $^3\text{He}^*$ will lead to the same degree of suppression of Penning ionization as that observed in $^4\text{He}^*$. If the inelastic rates prove to be sufficiently low, sympathetic cooling of $^3\text{He}^*$ by $^4\text{He}^*$ should lead to large Fermi-Bose mixtures [34].

In conclusion, we have observed strong evaporative cooling of a buffer gas loaded sample in the multi-partial-wave regime. This led to large clouds of ultracold metastable helium and is promising for the attainment of large Bose-Einstein condensates and quantum degeneracy of multispecies samples.

We acknowledge the assistance of Andrew Jayich and Matt Hummon. This work was supported by the NSF through the Harvard/MIT Center for Ultracold Atoms.

- [1] J. R. Anglin and W. Ketterle, *Nature (London)* **416**, 211 (2002).
- [2] M. R. Andrews *et al.*, *Science* **275**, 637 (1997).
- [3] J. R. Abo-Shaeer *et al.*, *Phys. Rev. Lett.* **94**, 040405 (2005).
- [4] S. Inouye *et al.*, *Nature (London)* **402**, 641 (1999).
- [5] L. Deng *et al.*, *Nature (London)* **398**, 218 (1999).
- [6] M. W. Zwierlein, J. R. Abo-Shaeer, A. Schirotzek, C. H. Schunck, and W. Ketterle, *Nature (London)* **435**, 1047 (2005).
- [7] K. W. Madison, F. Chevy, W. Wohlleben, and J. Dalibard, *Phys. Rev. Lett.* **84**, 806 (2000).
- [8] J. Stenger *et al.*, *Nature (London)* **396**, 345 (1998).
- [9] M. Greiner, O. Mandel, T. Esslinger, T. W. Hänsch, and I. Bloch, *Nature (London)* **415**, 39 (2002).
- [10] A. Robert *et al.*, *Nature (London)* **292**, 461 (2001).
- [11] F. Pereira Dos Santos *et al.*, *Phys. Rev. Lett.* **86**, 3459 (2001).
- [12] Z. Hu and H. J. Kimble, *Opt. Lett.* **19**, 1888 (1994).
- [13] A. Öttl, S. Ritter, M. Köhl, and T. Esslinger, *Phys. Rev. Lett.* **95**, 090404 (2005).
- [14] H. J. Kimble, M. Dagenais, and L. Mandel, *Phys. Rev. Lett.* **39**, 691 (1977).
- [15] M. Schellekens *et al.*, *Science* **310**, 648 (2005).
- [16] N. Herschbach, P. Tol, A. Tychkov, W. Hogervorst, and W. Vassen, *J. Opt. Soc. Am. B* **5**, S65 (2003).
- [17] J. D. Weinstein, R. deCarvalho, C. I. Hancox, and J. M. Doyle, *Phys. Rev. A* **65**, 021604(R) (2002).
- [18] C. I. Hancox, S. C. Doret, M. T. Hummon, L. Luo, and J. M. Doyle, *Nature (London)* **431**, 281 (2004).
- [19] J. D. Weinstein, R. deCarvalho, T. Guillet, Br. Friedrich, and J. M. Doyle, *Nature (London)* **395**, 148 (1998).
- [20] D. Egorov *et al.*, *Eur. Phys. J. D* **31**, 307 (2004).
- [21] J. G. E. Harris *et al.*, *Europhys. Lett.* **67**, 198 (2004).
- [22] I. Y. Fugol, O. N. Grigorashchenko, and D. A. Myshkis, *Sov. Phys. JETP* **33**, 227 (1971).
- [23] J. M. Doyle *et al.*, *J. Opt. Soc. Am. B* **6**, 2244 (1989).
- [24] D. M. Harber, J. M. McGuirk, J. M. Obrecht, and E. A. Cornell, *J. Low Temp. Phys.* **133**, 229 (2003).
- [25] L. Cai, B. Friedrich, and J. M. Doyle, *Phys. Rev. A* **61**, 033412 (2000).
- [26] J. D. Weinstein, Ph.D thesis, Harvard University, 2002 (unpublished).
- [27] G. V. Shlyapnikov, J. T. M. Walraven, U. M. Rahmanov, and M. W. Reynolds, *Phys. Rev. Lett.* **73**, 3247 (1994).
- [28] P. O. Fedichev, M. W. Reynolds, U. M. Rahmanov, and G. V. Shlyapnikov, *Phys. Rev. A* **53**, 1447 (1996).
- [29] W. Petrich, M. H. Anderson, J. R. Ensher, and E. A. Cornell, *Phys. Rev. Lett.* **74**, 3352 (1995).
- [30] K. B. Davis, M.-O. Mewes, M. A. Joffe, M. R. Andrews, and W. Ketterle, *Phys. Rev. Lett.* **74**, 5202 (1995).
- [31] T. Esslinger, I. Bloch, and T. W. Hänsch, *Phys. Rev. A* **58**, R2664 (1998).
- [32] Vim Vassen (private communication).
- [33] S. V. Nguyen *et al.*, *Phys. Rev. A* **71**, 025602 (2005).
- [34] A. S. Dickinson *et al.*, *J. Phys. B* **37**, 587 (2004).